GeoVirtual 2020 September 14-16
Resilience and Innovation

# Wellbore stability of highly deviated well intervals for large-diameter boreholes

Javad Someehneshin[a], Zijian Li[a], Weizhou Quan[a], Abdelsalam Abugharara[a,b] & Stephen Butt[a]
[a]*Memorial University of Newfoundland, St. John's, Newfoundland and Labrador, Canada,*
[b]*Sebha University, Sebha, Libya*
*Department of Process Engineering – the University of Newfoundland, St. John's, Newfoundland and Labrador, Canada*

ABSTRACT
In this paper, the analytical study, and the Discrete Element Method (DEM) simulation were conducted to evaluate the wellbore stability of steeply dipping mining utilizing various wellbore failure criteria. Mining site data of surface and subsurface in-situ stress, and rock mechanics properties were collected to support the study. The dimensions of the studied wellbore were 100m maximum depth, 1.3m maximum diameter, and 45 degrees inclination. The wellbore rock failure was analyzed, and the critical wellbore pressure after drilling in four essential azimuths (i.e. 0°, 90°, 180°, and 270°) using pure water was calculated. The results of the individual and the analytical-DEM coupled study demonstrated the wellbore stability.

RÉSUMÉ
Dans cet article, une étude analytique et une simulation de la méthode des éléments discrets (DEM) ont été menées pour évaluer la stabilité des puits de forage à forte inclinaison en utilisant divers critères de défaillance des puits de forage. Des données sur le site minier des propriétés in situ et des contraintes in situ et de mécanique des roches ont été recueillies à l'appui de l'étude. Les dimensions du puits de forage étudié étaient de 100 m de profondeur maximum, 1,3 m de diamètre maximum, 45 degrés d'inclinaison. La rupture de la roche de forage a été analysée, la pression critique de forage après le forage dans quatre azimuts essentiels (c.-à-d. 0o, 90o, 180o et 270o) en utilisant de l'eau pure a été calculée. Les résultats de l'individu et de l'étude couplée à l'analyse DEM ont approuvé la stabilité du puits de forage.

## 1 INTRODUCTION

The conventional development of steeply dipping narrow vein ore bodies (SDNVOB) is always a challenge due to extensive costs, high environmental impacts, and higher risk exposure. As an efficient alternative, the drilling method is introduced to overcome such challenges. In this concept, the SDNVOB will be crushed and transported to the surface in the process of directional drilling. The stability of the wellbores during and after drilling is critical for the safety of the hanging wall in highly deviated intervals of narrow vein mining and, therefore, requires intensive analysis to be maintained. In the mining industry, the occurrence of wellbore stability problems are frequent, leading to increasing drilling costs and overall non-operational time.

To ensure the wellbore stability, several factors must be considered including rock mechanical properties, wellbore trajectory, pore pressure, drilling fluid and pore fluid chemicals, temperature, time, mud weight and principal far-field stresses. Moreover, the wellbore formation bedding and natural fracture discontinuities and spacings as well as the influx of the drilling mud into these fractures could initiate the instability in rock masses. (Aoki et al., 1994; Chen et al., 1998; Last et al., 1995; Okland and Cook, 1998). The borehole diameter is another main parameter that affects the stability of the wellbore. According to the wellbore stability definition, as long as the wellbore and the drill bit have the same diameter and the drill bit keeps its shape constant, the well will be stable. Zhou et al. (1996) studied the deviated wellbore based on principal horizontal stress and reported that an inclined wellbore can be more stable than a vertical one when $\sigma_v > \sigma_H, \sigma_h$ (extensional stress regime).

Nowadays, the open stope mining method with a simple structure is widely used. This method grants simple investor operation, high production efficiency, small dilution and low cost. However, the over break and dilution caused by the stope hanging wall (HW) will damage the activity and economy of underground mines. Therefore, the efficiency of open stope mining is

generally determined by the capacity with minimal dilution to achieve the maximum extraction (Villaescusa, 2004). It is important to predict HW stability precisely and understand its influencing variables to prevent HW instability and support stable stope design. Wellbore stability requires a proper balance between the uncontrollable factors of earth stresses, rock strength, and pore pressure, wellbore fluid pore pressure, wellbore fluid pressure, and mud chemical composition (J.B. Cheatham Jr. 1984).

Several methods have been developed for the study of HW stability. Mathews et al. (1980) proposed a stability graph approach based on the Mathews stability number and the hydraulic radius to estimate HW stability. The stability of the wellbores during and after drilling is critical in narrow vein mining. In particular, the hanging wall must be stable to avoid wall collapse during drilling caused by inclination and the gravity force. The numerical method calculates the stress around the wellbore in different distances and different azimuths by using a failure criterion, the wellbore stability can be examined.

The support of the hanging wall in inclined wells is fundamental to the operation and safety of the mine site and areas. Bolting is the primary method of support in many modern mines in the USA and Australia. However, in some cases and for several reasons, rock bolts alone may not be sufficient to support the hanging wall, and secondary support must be installed.

Freezing (if there is water) or cement can be used, however, for the majority of the slopes and hanging walls, the installation of (Mega long bolts) cable bolts is the standard and most effective method of support.

The discrete element method (DEM) simulation is a good method to estimate the stress condition in a wellbore stability study. It has the advantage of monitoring the stress of every particle in the model, and therefore provides a more precise result.

For the wellbore instability, distributed stress, and rock strength, two major failure modes can be observed including shear and tensile failures. Shear fractures occur because of wellbore fluid pressure. Tensile fractures occur as a result of the excessive wellbore fluid pressure which has applied parallel to the maximum horizontal stress (σ H-Max). This paper studied the stresses around the wellbores in different locations and analyzes their impact on the wellbore stability utilizing a numerical analysis and DEM simulation. A failure criterion has also been applied after calculating the stress around the wellbore to examine the wellbore stability.

## 2 THEORETICAL METHOD

Underground formation is always under stress situations, mostly because of overburden and tectonic stresses. Stressed and solid material is removed when a well is drilled. During drilling, a concentration of stresses around the wellbore will be induced, which may cause the instability in the wellbores. Therefore the borehole will be supported only by the pressure of the mud or fluid in the bore. Since this support is not exactly the same as the extracted rock and in situ formation stresses, a stress redistribution will occur around the well. In this situation, failure may happen as the stress redistribution might lead to deviatoric stresses higher than the formation support.

If we consider the wellbore as a cylindrical shape, in order to examine the stresses in the rock surrounding a borehole, the stresses and strains in cylindrical coordinates need to be expressed. The stresses of any identified point by r, θ, and z coordination are denoted to radial stress ( $\sigma_r$), tangent stress ($\sigma_\theta$), axial stress ($\sigma_z$), and shear stress between them are $\tau_{r\theta}, \tau_{rz}, and\ \tau_{\theta z}$, respectively.

### 2.1 Well Control and In-Situ Stress

Well control is a procedure in drill planning to prevent unwanted conditions, such as kick and wellbore integrity. The kick occurs when the formation fluids enter the wellbore, and the wellbore integrity is the wellbore failure by fracturing. Both kick and well integrity are related to the bottom hole pressure (BHP). When the BHP is less than formation pore pressure, the kick will happen, and when BHP is greater than formation fracture pressure, the wellbore fracturing is expected.

In-situ stress is the natural and local stress within a rock mass formation, and it defines the quantity and direction of compression that is being applied to a rock at a specific location. It is a property of rock mass studied by trenchless construction planners in order to assess potential geotechnical challenges. Most *in-situ* stresses are caused by the body forces (gravity).

The pressure of the drilling fluid ($P_{mud}$) in the annulus of the wellbore depends on several factors such as hydraulic mud pressure, annular friction pressure (AFP), and dynamic pressure fluctuations (surge pressure & swab pressure). To stabilize the wellbore while drilling, mud pressure must be larger than formation pore pressure and less than formation fracture pressure.

### 2.2 Wellbore Wall Failure Modes

Minimum well pressure ($P_{w\text{-}min}$) and maximum well pressure ($P_{w\text{-}max}$) or fracture pressure are two essential parameters that must be measured to study wellbore stability. $P_{w\text{-}min}$ is generally less than pore pressure, and for weak formations and high *in-situ* stress zone (deep formations), it has a significant role in most drilling design.

When the stress distribution around the wellbore is determined, the wellbore stability can be assessed based on a failure criterion. There are two kinds of failure modes in this context. When the bottom hole pressure (BHP) is greater than maximum well pressure, tensile fractures will occur parallel to the maximum horizontal stress$\sigma_H$. If the BHP is less than minimum well pressure, shear fractures or compressive fractures will develop parallel to the minimum horizontal stress $\sigma_h$(FJÆR et al. 2008).

## 2.3 Transformation Formulas

The application of transformation formulas can make the evaluation of the stresses around the wellbore easier. The *in situ* principal stresses define a coordinate system that we denote as (x', y', z') indicated in Figure 1. We take $\sigma_v$ to be parallel to z', $\sigma_H$ to be parallel to x', and $\sigma_h$ to be parallel to y'.

For inclined wellbore, the directions of the wellbore axis and the gravity are not parallel. Thus, a second coordinate system (x, y, z) is introduced. In this coordinate system, the z-axis points along the axis of the hole, the x-axis points towards the lowermost radial direction of the hole, and the y-axis is horizontal (FJÆR et al. 2008).

$$\sigma_r = \frac{\sigma_x^\circ + \sigma_y^\circ}{2}\left(1 - \frac{R_w^2}{r^2}\right) + \frac{\sigma_x^\circ - \sigma_y^\circ}{2}\left(1 + 3\frac{R_w^4}{r^4} - 4\frac{R_w^2}{r^2}\right)\cos 2\theta + \tau_{xy}^\circ\left(1 + 3\frac{R_w^4}{r^4} - 4\frac{R_w^2}{r^2}\right)\sin 2\theta + p_w\frac{R_w^2}{r^2} \quad [1]$$

$$\sigma_\theta = \frac{\sigma_x^\circ + \sigma_y^\circ}{2}\left(1 + \frac{R_w^2}{r^2}\right) - \frac{\sigma_x^\circ - \sigma_y^\circ}{2}\left(1 + 3\frac{R_w^4}{r^4}\right)\cos 2\theta - \tau_{xy}^\circ\left(1 + 3\frac{R_w^4}{r^4}\right)\sin 2\theta - p_w\frac{R_w^2}{r^2} \quad [2]$$

$$\sigma_z = \sigma_z^\circ - \nu_{fr}\left[2\left(\sigma_x^\circ - \sigma_y^\circ\right)\frac{R_w^2}{r^2}\cos 2\theta + 4\tau_{xy}^\circ\frac{R_w^2}{r^2}\sin 2\theta\right] \quad [3]$$

$$\tau_{r\theta} = \frac{\sigma_y^\circ - \sigma_x^\circ}{2}\left(1 - 3\frac{R_w^4}{r^4} + 2\frac{R_w^2}{r^2}\right)\sin 2\theta + \tau_{xy}^\circ\left(1 - 3\frac{R_w^4}{r^4} + 2\frac{R_w^2}{r^2}\right)\cos 2\theta \quad [4]$$

$$\tau_{\theta z} = \left(-\tau_{xz}^\circ \sin\theta + \tau_{yz}^\circ \cos\theta\right)\left(1 + \frac{R_w^2}{r^2}\right) \quad [5]$$

$$\tau_{rz} = \left(\tau_{xz}^\circ \cos\theta + \tau_{yz}^\circ \sin\theta\right)\left(1 - \frac{R_w^2}{r^2}\right) \quad [6]$$

Where:

$$\sigma_x^\circ = l_{xx'}^2\sigma H + l_{xy'}^2\,\sigma h + l_{xz'}^2\sigma v \quad [7]$$

$$\sigma_y^\circ = l_{yx}^2\,\sigma H + l_{yy'}^2\sigma h + l_{yz}^2\,\sigma v \quad [8]$$

$$\sigma_z^\circ = l_{zx'}^2\sigma H + l_{zy'}^2\sigma h + l_{zz'}^2\sigma v \quad [9]$$

$$\tau_{xy}^\circ = l_{xx'}l_{yx'}\sigma H + l_{xy'}l_{yy'}\sigma h + l_{xz'}l_{yz'}\sigma v \quad [10]$$

$$\tau_{yz}^\circ = l_{yx'}l_{zx'}\sigma H + l_{yy'}l_{zy'}\sigma h + l_{yz'}l_{zz'}\sigma v \quad [11]$$

$$\tau_{zx}^\circ = l_{zx'}l_{xx'}\sigma H + l_{zy'}l_{xy'}\sigma h + l_{zz'}l_{xz'}\sigma v \quad [12]$$

$\sigma_r$ is the radial stress; $\sigma_\theta$ is the tangent stress; $\sigma_z$ is the axial stress, $\tau_{r\theta}, \tau_{rz}$ and $\tau_{\theta z}$ are the shear stress between planes, respectively. $Rw$ is the wellbore radius, $r$ is the distance from the wellbore, $\theta$ is the inclination angle, and $\nu_{fr}$ is the Poisson ratio. $\sigma_v$ is normal vertical stress, $\sigma_H$ is maximum horizontal stress, and $\sigma_h$ is minimum horizontal stress. $l_{ij'}$ is the cosine of the angle between the i-axis and the j'-axis.

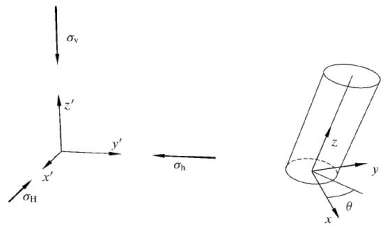


Figure 1. Schematic view of the axis on the wellbore

## 2.4 Critical Wellbore Pressure

A Closed-form Solution for calculating critical wellbore pressure was conducted. Using the transformed formula that can be found in many references, and the in-situ stresses were transformed into the wellbore coordination system. 23 °inclination was considered for the wellbore and $\sigma_x$ , $\sigma_y$ , $\sigma_{zz}$ , $\tau_{xy}$ , $\tau_{yz}$, and $\tau_{zx}$ were calculated, where $\sigma_{zz}$ is parallel to the direction of the wellbore and $\sigma_x$ and $\sigma_y$ act orthogonal to the wellbore direction. The modified Lade criterion is used to calculate the critical wellbore pressure ($P_w$) that prevents the instability of the wellbores.

$$P\_w = (B - \sqrt{C})/2A \quad [13]$$

$$A = \sigma_z + S_1 - P_P \quad [14]$$

$$B = A\sigma_{\theta^n} - \tau_{\theta^z}^2 \quad [15]$$

$$C = B^2 - 4A\{D - (S_1 - P_P)[A(\sigma_{\theta^n} + S_1 - P_P) - \tau_{\theta^z}]\} \quad [16]$$

$$D = (\sigma_{\theta^n} + \sigma_z + 3S_1 - 3P_P)^3/(27 + \eta) \quad [17]$$

$$\sigma_{\theta^n} = \sigma_x + \sigma_y - 2(\sigma_x - \sigma_y)cos2\theta - 4\tau_{xy}sin2\theta \quad [18]$$

$$\sigma_z = \sigma_{zz} - \mu\left[2(\sigma_x - \sigma_y)cos2\theta - 4\tau_{xy}sin2\theta\right] \quad [19]$$

$$\tau_{\theta^z} = 2(\tau_{yz}cos\theta - \tau_{zx}sin\theta) \quad [20]$$

The critical wellbore pressure must be compensated by mud weight. When the critical wellbore pressure increases, the mud weight must be increased to provide sufficient pressure to the wellbore walls to prevent instability. In this study, the critical wellbore pressure after drilling in four essential azimuths Includes 0, 90, 180, and 270 degrees from the x-axis, was calculated.

Table 1 shows the critical wellbore pressure for this case study in four important azimuths. At the top of the wellbore, the critical wellbore pressure is -9.653, and at the bottom of the wellbore, it is -8.72. It is clear when the critical wellbore pressure is negative, the wellbore is stable, and any mud with the lowest density can be used as drilling fluid.

Table 1- critical wellbore pressure

| Azimuth | 0 | 90 | 180 | 270 |
|---|---|---|---|---|
| Bottom | -8.72 | -8.72 | -8.72 | -8.72 |
| Top | -9.65 | -9.65 | -9.65 | -9.65 |

## 3 CASE STUDY: WELLBORE STABILITY ASSESSMENT IN THE TARGET MINING ZONE

In the mining zone, the prospect consists of three quartz veined zones up to 1m to 2m thick, exposed over 300m. The dipping angle varies from 65 to 72 degrees from horizontal. Fine-grained, mafic volcanic, and gabbroic intrusive rocks host the veins. The veins are spatially associated with a north-northeast-trending topographic lineament that continues for several kilometres to the north. Mineralization has been traced for approximately 100m and is open to the east, west, and down dip. For this mining zone, the development plan is to excavate the vein by sequential borehole drilling mining method. Pure water is planned to be used as mud for the drilling. The drill hole depth could reach 100m. Thus, wellbore stability is of great importance in this project.

### 3.1 Wellbore Conditions in the Target Mining Zone

In this study, the target depth of the wellbores is 100m, and the radius of the wellbore ($r_w$) is 0.65m. As the vein has a variable inclination, we studied inclination from 18 to 23 °and 45 °and the depth from zero (surface) to 100m with one meter interval. The stress distribution around the wellbore is studied every 10 °from zero to 360 °. Several essential distances (R) were selected for the calculation, $r_w$ (0.65m), $5r_w$ (3.25m), $10r_w$ (6.5m), and 10m. In general, it is believed that the wellbore has very little influence on the stress distribution further than $5r_w$ (3.25m) away from the wellbore center. Figure 2 shows the different distances from $r_w$ to 10m in different colours. Black is the wellbore, brown presents the stresses exactly on the wellbore wall; orange is the stress in $5r_w$ distance, yellow on $10r_w$ and green on 10m distance.

The results only show the specific 23 °inclination at $R=r_w$=0.65m since the qualitative behaviour of stresses for the mentioned inclinations and distances are almost the same.

Each time, the distance (R) is considered constant and by increasing the depth from zero to 100m, $\sigma_r, \sigma_\theta, \sigma_z, \tau_{r\theta}, \tau_{rz}, \text{and } \tau_{\theta z}$ are calculated by transformation formulas [1] to [6] for every 10 °around the wellbore. Pw-min and Pw-max from the depth of zero to 100m are calculated. Table 2 shows the input data used to analyze the stress around the well.

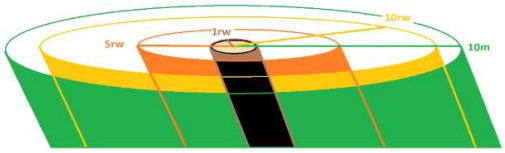


Figure 2. Schematic view of a well and the studied stresses around it on different distance

Table 2. Geomechanics parameters of the vein used for analyzing stresses

| Characteristics | Value | Unit |
|---|---|---|
| Rock density | 2480 | $Kg/m^3$ |
| Unconfined compressive strength (UCS) of the rock | 94 | MPa |
| Poisson ratio | 0.25 | Unit less |
| Internal friction angle | 55 | degree |
| Cohesion | 15 | MPa |

### 3.2 Joint and GSI (geological strength index) of the host rock

Figure 3 shows the blocky host rock, which is a mafic rock with a good quality surface area. Table 3 summarizes more information such as RQD, and GSI of the host rock.

Table 3- Rock mass characteristic of the host rock

| Joint set | 1 | 2 |
|---|---|---|
| Average Specing | 42.75cm | 16.2cm |
| Ja | 3 | 3 |
| Jr | 1.5 | 1.5 |
| Jv | 8.5 | |
| RQD | 88.7 | |
| GSI | 61.6 | |
| Mi (for Quartzite)* | 20 | |

* Marinos, P., and Hoek, H., GSI: A GEOLOGICALLY FRIENDLY TOOL FOR ROCK MASS STRENGTH ESTIMATION

Figure 3- the host rock of the case study

## 4 NUMERICAL RESULTS

### 4.1 $P_{w\text{-}min}$ Versus $P_{w\text{-}max}$

Figure 4 shows the minimum well pressure ($P_{w\text{-}min}$) and maximum well pressure ($P_{w\text{-}max}$) versus depth. The upper line is the $P_{w\text{-}max}$, and the lower line is the $P_{w\text{-}min}$. As expressed before, if the stresses around the wellbore are between these two lines, the wellbore will be stable. If the pressure is beyond this range, the well will fail. In the next step, radial, tangent, axial, and shear stresses surrounding the hole are calculated. If these stresses are higher than minimum well pressure and lower than maximum well pressure, the well is stable.

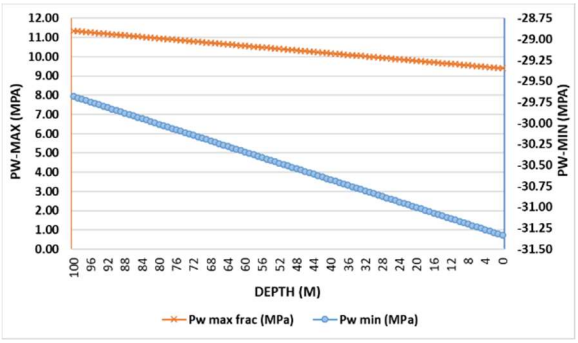


Figure 4. Comparison of the minimum well pressure (Pw-min) and maximum well pressure (Pw-max) as a function of depth

### 4.2 Failure Criterion

Mohr-Coulomb and Drucker Prager criterion is the most famous failure criteria used for analyzing wellbore stability, however, they do not consider the effect of intermediate principal stress on rock strength. Modified Lade criterion can provide a closed-form solution for critical wellbore pressure and, consequently, the critical mud weight. It also reflects the influence of intermediate principal stress. In this paper, the Mohr-Coulomb, Ducker Parger (Inner circle, Middle circle, and outer circle), the Modified Lade criterion, and the Modified Hoek and Brown are analyzed. The summary of the failure criterion can be found in the results section. However, the Modified Hoek and Brown failure criterion will be discussed in detail.

### 4.3 Modified Hoek and Brown Criterion

Hoek and Brown 1980 developed a failure criterion to estimate jointed rock mass strength. The limitations were derived in 1983 using laboratory triaxial tests on samples of intact rocks. The modified Hoek and Brown criterion was later presented for heavily jointed rock masses.

The GSI was developed by Hoek 1994 and Hoek et al. 1995 In order to link engineering geology observations in the field and the Modified Hoek & Brown criterion. GSI is the rock mass characterization system based on the structure and the condition of the joints.

$$\sigma 1 = \sigma 3 + \sigma ci\ (mb\ \ \sigma 3/\sigma ci\ + s)\text{^}a \quad [21]$$

$$mb = mi\ \ \exp[(GSI - 100)/(28 - 14D)] \quad [22]$$

$$s = \exp[(GSI - 100)/(9 - 3D)] \quad [23]$$

$$a = 1/2 + 1/6(e\text{^}(-GSI/15) - e\text{^}(-20/3)) \quad [24]$$

Where $\sigma_1$ and $\sigma_3$ are the major and minor principal stresses, respectively,$\sigma_{ci}$ is the unconfined compressive strength, and mi is a material constant for the intact rock. D is a factor that represents the disturbance degree used for damage by blasting, and for this study, it is considered as zero since the wells are drilled and no explosives material were used.

### 4.4 Failure Criterion Results

For all of the mentioned failure criteria, there is a failure index formula that uses principal stress, internal friction angle, pore pressure, and cohesion to evaluate the stability of the wellbore. If the failure index is less than zero (FI<0), then the wellbore fails. The equations are not presented in this paper as they can be found in many references (such as FJÆR et al. 2008).

The failure index of all failure criterion such as Mohr-Coulomb, Ducker-Prager, Modified Lade, and modified Hoek-Brown criterion was calculated from the top to the bottom of the wellbore at every one-meter intervals, and all indicate that the FI is greater than Zero (FI>0) and the wellbore is stable from the surface to the bottom of the well. Table 4 summarizes the FI for different failure criteria. Note that the bottom of the well shows a greater FI than the top of the well, and this is due to the horizontal stresses that act as confining compressive stress (CCS). By increasing the depth, the magnitude of the horizontal stresses would increase and consequently the CCS will increase.

Table 4- Failure index for different failure criterion

| Failure Criterion | FI at the Bottom of the well | FI at the Top of the well |
|---|---|---|
| Mohr-Coulomb | 100.4 | 95.15 |
| Ducker-Prager (inner circle) | 9.76 | 9.06 |
| Ducker-Prager (Middle circle) | 1.12 | 0.42 |
| Ducker-Prager (Outer circle | 1.99 | 0.74 |
| Modified Lade | 147.28 | 147.33 |
| Modified Hoek-Brown | 29.17 | 11.01 |

## 4.5 Stress Between $P_{w\text{-}min}$ & $P_{w\text{-}max}$

Figure 5 shows the radial stress (around the well $R=r_w=0.65m$), $P_{w\text{-}min}$, and $P_{w\text{-}max}$. The upper surface is Pw-max, and the lower surface is Pw-min. The radial stress is the middle surface. Since the range of the stresses in $P_{w\text{-}min}$ and $P_{w\text{-}max}$ is much higher than radial stress, the radial stresses are shown as a small picture on the upper left. It is clear that the radial stress is between $P_{w\text{-}min}$ and $P_{w\text{-}max}$, and as previously mentioned, the wellbore is stable.

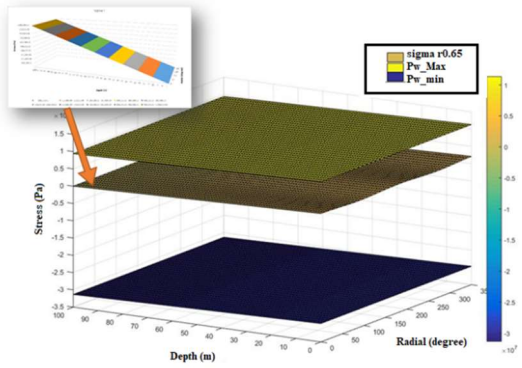


Figure 5. The radial stress (around the well $r=R_w=0.65m$), $P_{w\text{-}min}$, and $P_{w\text{-}max}$

Figures 6 to 10 show the tangent stress, axial stress, shear stress of the radial and tangent planes, shear stress of the tangent and axial planes, and shear stress of the radial and axial planes (around the well $r=R_w=0.65m$), respectively, as well as $P_{w\text{-}min}$, and $P_{w\text{-}max}$. The insets on the upper left corner of each figure show the magnified stresses. The figures imply that the same principals discussed above continue to apply and that the wellbore is stable.

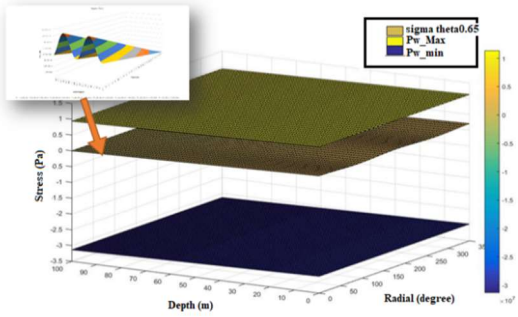


Figure 6. The tangent stress (around the well $r=R_w=0.65m$) $P_{w\text{-}min}$, and $P_{w\text{-}max}$

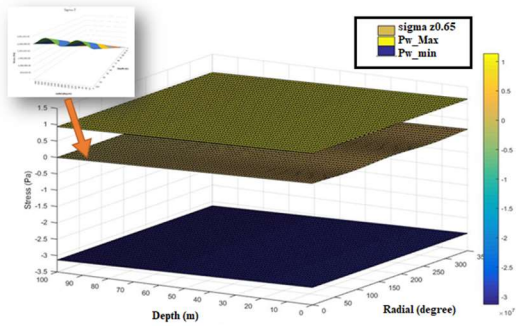


Figure 7. The axial stress (around the well $r=R_w=0.65m$), $P_{w\text{-}min}$, and $P_{w\text{-}max}$

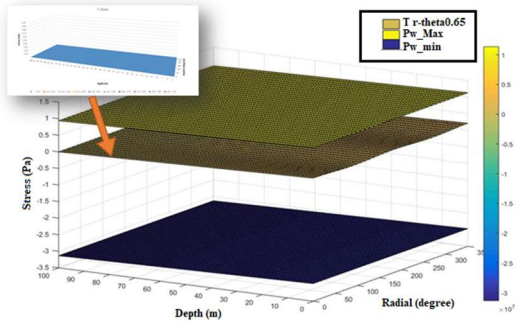


Figure 8. The shear stress of the radial and tangent planes (around the well $r=R_w=0.65m$), $P_{w\text{-}min}$, and $P_{w\text{-}max}$

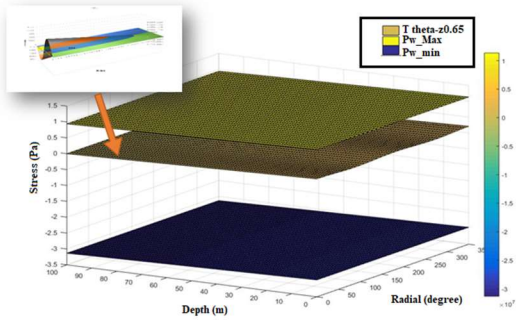


Figure 9. The shear stress of the tangent and axial planes (around the well $r=R_w=0.65m$), $P_{w\text{-}min}$, and $P_{w\text{-}max}$

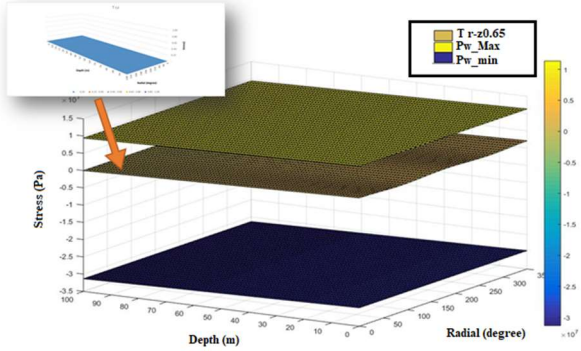


Figure 10. The shear stress of the radial and axial planes (around the well $r=R_w=0.65m$), $P_{w\text{-}min}$, and $P_{w\text{-}max}$

## 5 DISCRETE ELEMENT METHOD (DEM) SIMULATION OF WELLBORE STABILITY

DEM is a numerical method for calculating the dynamics of discrete elements to obtain the macro property of a target sample. DEM was originally introduced to analyze problems in rock mechanics by Cundall (1971). Today, DEM has been applied in many other fields (Glamheden et al., 2004; Szymakowski, 2004; Konietzky et al., 2004). DEM also has the potential to carry out the wellbore stability analysis because it can trace the dynamics of every particle in the model. In this study, Particle Flow Code 2D (PFC2D) software is used for the DEM simulation.

Before the start of the DEM simulation, a rock model should be created and calibrated. By toning the micro property parameters, the macro property of the rock model should match the rock properties measured in the lab. Then, the rock model is created using the calibrated micro property parameters. After the model generation, the in-situ stresses (maximum and minimum horizontal stresses) are applied to the boundaries of the model. The model reaches stress equilibrium after running a long time.

A wellbore is 'drilled' in the middle of the model. Mud pressure is applied on the surface of the wellbore. The DEM model is shown in Figure 11. Then, the model starts to run the force-displacement calculation over time. The stress condition of particles at the selected location is monitored and output to the log. The stress distribution at 100m depth and $R=r_w$=0.65m is presented and compared with the theoretical result.

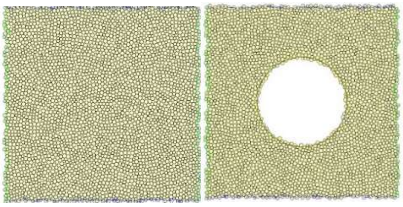

Figure 11 DEM rock model reaches equilibrium with in-situ stress (left) and wellbore drilled in the center (right).

It is observed that the average DEM result agrees with the theoretical result. On the other hand, the maximum stresses in the DEM result tend to be higher than the theoretical calculation result. This is because the stress is unevenly distributed in DEM simulations, which is different from the theotical result. At some points, the stress can be notably higher than the nearby area. The stress concentration is well monitored in DEM simulation. There is no micro fracture observed in the DEM simulation, which suggests that the wellbore is at safe condition. This result agrees with the theoretical result.

Table 5 Comparison of between theoretical result and DEM simulation result parameters of the vein used for analyzing stresses at 100m depth and R=rw=0.65m

| Azimuth (degree) | Radial stress (Theoretical) (MPa) | Radial stress (Maximum value in DEM) (MPa) | Radial stress (Average value in DEM) (MPa) |
|---|---|---|---|
| 0 | 0.05 | 0.31 | 0.07 |
| 90 | 0.21 | 0.79 | 0.20 |
| 180 | 0.07 | 0.42 | 0.08 |
| 270 | 0.23 | 0.83 | 0.25 |
| Azimuth (degree) | Tangent stress (Theoretical) (MPa) | Tangent stress (Maximum value in DEM) (MPa) | Tangent stress (Average value in DEM) (MPa) |
| 0 | 0.08 | 0.17 | 0.10 |
| 90 | 0.25 | 0.32 | 0.27 |
| 180 | 0.11 | 0.21 | 0.09 |
| 270 | 0.28 | 0.35 | 0.28 |

## 6 CONCLUSIONS

For a well to be stable during and after drilling, applied stresses must be studied at different distances. The effective distance is usually considered five times of the well radios. This paper analyzed the radial stress, tangent stress, axial stress, shear stresses on these planes on the edge of the wellbore, five times of the well radios, ten times of the radios, and ten meters from the wellbore.

Since the inclination of the wellbore under study is 23°, all stresses mentioned above were studied at 18, 19, 20, 21, 22, 23, and 45 °. These stresses were also calculated from surface to 100 m depth at each 1 m depth increment, from wellbore edge to 10 m radial distance, and at each 10 degrees increment from 0° to 360°.

For the efficient drilling process applied in steeply dipping mining and optimal stable hanging walls of wellbores, stresses must be studied at various intervals of depth and radius. For effective radial stress analysis, the distance is usually considered as five times of the well radius. Moreover, tangent, axial, and shear stresses on planes of the edge of the wellbore involving different scenarios of five times of the well radios, ten times of the radios, and ten meters from the wellbore were determined.

The results of the stress analysis by the analytical and DEM methods can be summarized as:

The radial and axial stresses on the edge of the wellbore are linear and will increase by increasing the depth. However, this trend at five times the well radios and more converts to a sinusoidal shape and fluctuate every 90 degrees, while the entire style is a rising trend.

The tangent stresses at the wellbore edge, and five times the well radios and more is a sinusoidal shape and will increase by increasing the depth. This stress also has fluctuations every 90 degrees, but the entire style is a rising trend.

The shear stress of the radial and tangent planes is zero on the edge of the wellbore from the surface to

100m depth and all around the wellbore. However, this trend at five times the well radios and more converts to a sinusoidal shape and fluctuate every 90 degrees, while the entire style is a rising trend.

The shear stress of the tangent and axial planes on the edge of the wellbore has one periodic sinusoidal shape. This graph at zero and 180 degrees has zero value and at 90 and 270 degrees is maximum and negative maximum.

The shear stress of the radial and axial planes is zero on the edge of the wellbore from the surface to 100m depth and all around the wellbore. However, this trend at five times the well radios and more converts to a curve shape and has a peak at 180 degrees, while the entire style is a rising trend.

The average results of the DEM simulation agreed with the theoretical results. However, the maximum stress near the wellbore obtained by the DEM simulation is higher than that of the theoretical, suggesting that there was a stress concentration phenomenon. In the far-field region from the wellbore center, the stress concentration was decreased.

All Failure Criterion, the theoretical calculation results, and the DEM simulation result showed that all calculated stresses are between these two surfaces, and the wellbore is stable and safe up to 100m depth.

## 7 REFERENCES


Aoki, T., Tan, C.P., Bamford, W.E., 1994. Stability analysis of inclined wellbores in saturated anisotropic shales. 8th International Conference on Computer Methods and Advances in Geomechanics. Balkema, Rotterdam, pp. 2025– 2030.

Chen, X., Tan, C.P., Haberfield, C.M., 1998. A comprehensive practical approach for wellbore instability management. 1998 SPE International Conference and Exhibition. Beijing, China, pp. 623–638.

Cundall, P.A. (1971): A computer model for simulating progressive large scale movements in blocky rock systems, *proceedings of the symposium of the international society of rock mechanics, 1971*

FJÆR, E., HOLT, R.M., HORSRUD, P., RAAEN, A.M. & RISNES, R. 2008. Petroleum Related Rock Mechanics, 2nd ed., Amsterdam – Boston – Heidelberg – London – New York – Oxford Paris – San Diego – San Francisco – Singapore – Sydney – Tokyo

Glamheden, R., Hökmark, H., & Christiansson, R. (2004). Modeling creep in jointed rock masses, 1st International UDEC/3DEC Symposium: Numerical Modeling of Discrete Materials in Geotechnical Engineering. *Civil Engineering and Earth Science, Bochum, Germany.*

Henning, J. G., and Mitri, H. S. (2007). "Numerical modelling of ore dilution in blasthole stoping." Int. J. Rock Mech. Min. Sci., 44(5), 692–703

J.B. Cheatham Jr. (1984). "wellbore stability". Journal of Petroleum Technology. Society of Petroleum Engineers.

Kang, Y., Yu, M., Miska, S. Z., & Takach, N. (2009, January). Wellbore stability: A critical review and introduction to DEM. In *SPE Annual Technical Conference and Exhibition*. Society of Petroleum Engineers.

Konietzky, H., te Kamp, L., Groeger, T., & Jenner, C. (2004). Use of DEM to model the interlocking effect of geogrids under static and cyclic loading. *Numerical modeling in micromechanics via particle methods*, 3-12.

Last, N.C., Plumb, R., Harkness, R., Charlez, P., Alson, J., McLean, M., 1995. An integrated approach to evaluating and managing wellbore instability in the Cusiana field, Colombia, South America. SPE, 30646.

Mathews, K. E., Hoek, D. C., Wyllie, D. C., and Stewart, S. B. V. (1980). "Prediction of stable excavation spans for mining at depths below 1,000 meters in hard rock." DSS File No. 17SQ.23440-0-90210, Canada Centre for Mineral and Energy Technology, Ottawa.

Mawdesley, C., Trueman, R., and Whiten, W. J. (2001). "Extending the Mathews stability graph for open-stope design." Mini. Technol., 110(1), 27–39.

Okland, D., Cook, J.M., 1998. Bedding-related borehole instability in high-angle wellsSPE/ISRM EUROCK'98: Rock Mechanics in Petroleum Engineering, vol. 1. Trondheim, Norway, pp. 413–422.

Qi, C., Fourie, A., Ma, G., Tang, X., & Du, X. (2018). "Comparative study of hybrid artificial intelligence approaches for predicting hanging wall stability". Journal of Computing in Civil Engineering, 32(2), 04017086.

Stewart, P., and Trueman, R. (2003). "Applying the extended Mathews stability graph to stress relaxation, site-specific effects and narrow-vein stoping." Proc., 1st Australasian Ground Control in Mining Conf.— Ground Control in Mining: Technology and Practice, UNSW School of Mining Engineering, Sydney, Australia, 55–61.

Szymakowski, J. B. (2004, October). UDEC modeling of constant normal stiffness direct shear tests. In Numerical Modelling of Discrete Materials in Geotechnical Engineering, Civil Engineering and Earth Sciences: Proceedings of the First International UDEC/3DEC Symposium, Bochum, Germany, 29 September-1 October 2004 (p. 145). CRC Press.

Villaescusa, E. (2004). "Quantifying open stope performance." Proc., MassMin, Chilean Engineering Institute, Santiago, Chile, 96–104.

Zhou, S., Hillis, R., Sandiford. M., (1996): On the Mechanical Stability of Inclined Wellbores, SPE 28176, SPE Drilling & Completion. Volume 11, Number 2, June 1996. PP. 67-73